Title

Comprehensive genomic characterization of head and neck squamous cell carcinomas

Journal

Nature, 517(7536)

ISSN

0028-0836

Authors

Lawrence, Michael S

Sougnez, Carrie

Lichtenstein, Lee

et al.

Publication Date

2015-01-29

DOI

10.1038/nature14129

Peer reviewed

HHS Public Access

Author manuscript

Nature. Author manuscript; available in PMC 2015 July 29.

Published in final edited form as:

Nature. 2015 January 29; 517(7536): 576–582. doi:10.1038/nature14129.

Comprehensive genomic characterization of head and neck squamous cell carcinomas

The Cancer Genome Atlas Network *

Abstract

The Cancer Genome Atlas profiled 279 head and neck squamous cell carcinomas (HNSCCs) to provide a comprehensive landscape of somatic genomic alterations. We find that human papillomavirus-associated (HPV) tumors are dominated by helicase domain mutations of the oncogene *PIK3CA*, novel alterations involving loss of *TRAF3*, and amplification of the cell cycle gene *E2F1*. Smoking-related HNSCCs demonstrate near universal loss of *TP53* mutations and *CDKN2A* with frequent copy number alterations including a novel amplification of 11q22. A subgroup of oral cavity tumors with favorable clinical outcomes displayed infrequent CNAs in conjunction with activating mutations of *HRAS* or *PIK3CA*, coupled with inactivating mutations of *CASP8*, *NOTCH1* and wild-type *TP53*. Other distinct subgroups harbored novel loss of function alterations of the chromatin modifier *NSD1*, *Wnt* pathway genes *AJUBA* and *FAT1*, and activation of oxidative stress factor *NFE2L2*, mainly in laryngeal tumors. Therapeutic candidate alterations were identified in the majority of HNSCC's.

Introduction

HNSCCs impact ~600,000 patients per year worldwide [1]. They are characterized by phenotypic, etiologic, biologic, and clinical heterogeneity. Smoking is implicated in the rise of HNSCC in developing countries, while the role of HPV is emerging as an important factor in the rise of oropharyngeal tumors affecting non-smokers in developed countries [2]. Despite surgery, radiation, and chemotherapy, approximately half of all patients will die of the disease. Risk stratification for HNSCC is by anatomic site, stage, and histologic characteristics of the tumor. Except for HPV status, numerous molecular and clinical risk factors that have been investigated have limited clinical utility.

Published genome-wide profiling studies of HNSCC[3,4] are limited to single platforms. To generate an integrated genomic annotation of molecular alterations in HNSCC, The Cancer Genome Atlas (TCGA) has undertaken a comprehensive multi-platform characterization of 500 tumors with the *a priori* hypothesis of detecting somatic variants present in at least 5% of samples. Here, we report the results for analyses from the first 279 patients with complete data.

Samples and Clinical Data

The cohort is comprised primarily of tumors from the oral cavity (n=172/279, 62%), oropharynx (n=33/279, 12%), and laryngeal sites (n=72/279, 26%) (Section S1, Table S1.1, Data File S1.1). Most patients were male (n=203/279, 73%) and heavy smokers (mean pack

years = 511). Samples were classified as HPV positive using an empiric definition of >1000

centres, cancer genome characterization centres and genome data analysis centres. All data were released through the data coordinating centre. Project activities were coordinated by the National Cancer Institute and National Human Genome Research Institute project teams. We also acknowledge the following TCGA investigators who made substantial contributions to the project: C. V. W.(manuscript coordinator); V. W. (data coordinator); P. S. H., D. N. H. (analysis coordinators); Y. W. (DCC Representative); R. A., J. B., T. E. C., J. J. L., A. D. T., V. W., M. D. W. (clinical and HPV analysis); A. D. C. (DNA copy number analysis); J. Cho, A. H., M. Parfenov, M. D. W. (Mutation calling); L. C., L. Danilova (DNA methylation analysis); R. Bowlby, J. P. B., Z. C., H. Cheng., A. H., F. F. L., A. G., R., A. D., S., C. V. W. (miRNA sequence analysis); L. A. B., L. Diao, P. K., W. L., S. N., J. W. (RPPA analysis); L. A. B., L. Diao, S. R. J., P. K. K., V. W., M. D. W., N. Z. (mRNA sequence analysis); S. Benz, Z. C., R. L. F., S. N., C. R. P., N. Schultz, T. Y. S., C. V. W., V. W. (pathway analysis) A. E. N., J. R. G., D. N. H. (project chairs).

Author Information: The primary and processed data used to generate the analyses presented here can be downloaded by registered users from The Cancer Genome Atlas (https://tcga-data.nci.nih.gov/tcga/tcgaDownload.jsp, https://cghub.ucsc.edu/ and https://tcga-data.nci.nih.gov/docs/publications/XXXXXXXX/).

The authors declare no competing financial interests. Readers are welcome to comment on the online version of the paper.

Characterization, sequencing and analysis centers: BC Cancer Agency Adrian Ally, Miruna Balasundaram, Inanc Birol, Reanne Bowlby, Denise Brooks, Yaron S.N. Butterfield, Rebecca Carlsen, Dean Cheng, Andy Chu, Noreen Dhalla, Ranabir Guin, Robert A. Holt, Steven J.M. Jones, Darlene Lee, Haiyan I. Li, Marco A. Marra, Michael Mayo, Richard A. Moore, Andrew J. Mungall, A. Gordon Robertson, Jacqueline E. Schein, Payal Sipahimalani, Angela Tam, Nina Thiessen, Tina Wong; Harvard Medical School/ Brigham & Women's Hospital/MD Anderson Cancer Center Alexei Protopopov, Netty Santoso, Semin Lee, Michael Parfenov, Jianhua Zhang, Harshad S. Mahadeshwar, Jiabin Tang, Xiaojia Ren, Sahil Seth, Psalm Haseley, Dong Zeng, Lixing Yang, Andrew W. Xu, Xingzhi Song, Angeliki Pantazi, Christopher A. Bristow, Angela Hadjipanayis, Jonathan Seidman, Lynda Chin, Peter J. Park, Raju Kucherlapati; **The University of Texas MD Anderson Cancer Center** Rehan Akbani, Tod Casasent, Wenbin Liu, Yiling Lu, Gordon Mills, Thomas Motter, John Weinstein, Lixia Diao, Jing Wang, You Hong Fan; **University of Kentucky** Jinze Liu, Kai Wang; **University of North Carolina at Chapel Hill** J. Todd Auman, Saianand Balu, Thomas Bodenheimer, Elizabeth Buda, D. Neil Hayes, Katherine A. Hoadley, Alan P. Hoyle, Stuart R. Jefferys, Corbin D. Jones, Patrick K. Kimes, Yufeng Liu, J.S. Marron, Shaowu Meng, Piotr A. Mieczkowski, Lisle E. Mose, Joel S. Parker, Charles M. Perou, Jan F. Prins, Jeffrey Roach, Yan Shi, Janae V. Simons, Darshan Singh, Matthew G. Soloway, Donghui Tan, Umadevi Veluvolu, Vonn Walter, Scot Waring, Matthew D. Wilkerson, Junyuan Wu, Ni Zhao; **Broad Institute** Andrew D. Cherniack, Peter S. Hammerman, Aaron D. Tward, Chandra Sekhar Pedamallu, Gordon Saksena, Joonil Jung, Akinyemi I. Ojesina, Scott L. Carter, Travis I. Zack, Steven E. Schumacher, Rameen Beroukhim, Samuel S. Freeman, Matthew Meyerson, Juok Cho, Lynda Chin, Gad Getz, Michael S. Noble, Daniel DiCara, Hailei Zhang, David I. Heiman, Nils Gehlenborg, Doug Voet, Pei Lin, Scott Frazer, Petar Stojanov, Yingchun Liu, Lihua Zou, Jaegil Kim, Michael S. Lawrence, Carrie Sougnez, Lee Lichtenstein, Kristian Cibulskis, Eric Lander, Stacey B. Gabriel; **Baylor College of Medicine** Donna Muzny, HarshaVardhan Doddapaneni, Christie Kovar, Jeff Reid, Donna Morton, Yi Han, Walker Hale, Hsu Chao, Kyle Chang, Jennifer A. Drummond, Richard A. Gibbs, Nipun Kakkar, David Wheeler, Liu Xi; **Memorial Sloan-Kettering Cancer Center** Giovanni Ciriello, Marc Ladanyi, William Lee, Ricardo Ramirez, Chris Sander, Ronglai Shen, Rileen Sinha, Nils Weinhold, Barry S. Taylor, B. Arman Aksoy, Gideon Dresdner, Jianjiong Gao, Benjamin Gross, Anders Jacobsen, Boris Reva, Nikolaus Schultz, S. Onur Sumer, Yichao Sun, Timothy Chan, Luc Morris; **University of California Santa Cruz/Buck Institute** Joshua Stuart, Stephen Benz, Sam Ng, Christopher Benz, Christina Yau; Johns Hopkins University/Sidney Kimmel Comprehensive Cancer Center Stephen B. Baylin, Leslie Cope, Ludmila Danilova, James G. Herman; **University of Southern California** Moiz Bootwalla, Dennis T. Maglinte, Peter W. Laird, Timothy Triche, Jr., Daniel J. Weisenberger, David J. Van Den Berg.

Disease Working Group: Nishant Agrawal, Justin Bishop, Paul C. Boutros, Jeff P Bruce, Lauren Averett Byers, Joseph Califano, Thomas E. Carey, Zhong Chen, Hui Cheng, Simion I. Chiosea, Ezra Cohen, Brenda Diergaarde, Ann Marie Egloff, Adel K. El-Naggar, Robert L. Ferris, Mitchell J. Frederick, Jennifer R. Grandis, Yan Guo, Robert I. Haddad, Peter S. Hammerman, Thomas Harris, D. Neil Hayes, Angela BY Hui, J. Jack Lee, Scott M. Lippman, Fei-Fei Liu, Jonathan B. McHugh, Jeff Myers, Patrick Kwok Shing Ng, Bayardo Perez-Ordonez, Curtis R. Pickering, Michael Prystowsky, Marjorie Romkes, Anthony D. Saleh, Maureen A. Sartor, Raja Seethala, Tanguy Y. Seiwert, Han Si, Aaron D. Tward, Carter Van Waes, Daryl M. Waggott, Maciej Wiznerowicz, Wendell G. Yarbrough, Jiexin Zhang, Zhixiang Zuo.

Biospecimen Core Resource: International Genomics Consortium Ken Burnett, Daniel Crain, Johanna Gardner, Kevin Lau, David Mallery, Scott Morris, Joseph Paulauskis, Robert Penny, Candance Shelton, Troy Shelton, Mark Sherman, Peggy Yena; **Nationwide Children's Hospital** Aaron D. Black, Jay Bowen, Jessica Frick, Julie M. Gastier-Foster, Hollie A. Harper, Kristen Leraas, Tara M. Lichtenberg, Nilsa C. Ramirez, Lisa Wise, Erik Zmuda.

Data Coordinating Center: Julien Baboud, Mark A. Jensen, Ari B. Kahn, Todd D. Pihl, David A. Pot, Deepak Srinivasan, Jessica S. Walton, Yunhu Wan.

Project Office: Robert Burton, Tanja Davidsen, John A. Demchok, Greg Eley, Martin L. Ferguson, Kenna R. Mills Shaw, Bradley A. Ozenberger, Margi Sheth, Heidi J. Sofia, Roy Tarnuzzer, Zhining Wang, Liming Yang, Jean Claude Zenklusen.

Tissue Source Sites: Analytical Biological Services Charles Saller, Katherine Tarvin; **Fred Hutchinson Cancer Research Center** Chu Chen; **Georgia Regents University** Roni Bollag, Paul Weinberger; **Greater Poland Cancer Centre** Wojciech Golusiński, Paweł Golusiński, Matthiew Ibbs, Konstanty Korski, Andrzej Mackiewicz, Wiktoria Suchorska, Bartosz Szybiak, Maciej Wiznerowicz; **International Genomics Consortium** Ken Burnett, Erin Curley, Johanna Gardner, David Mallery, Robert Penny, Troy Shelton, Peggy Yena; **Indiana University Simon Cancer Center** Christina Beard, Colleen Mitchell, George Sandusky; **Johns Hopkins University** Nishant Agrawal, Julie Ahn, Justin Bishop, Joseph Califano, Zubair Khan; **Princess Margaret Cancer Centre** Jeff P Bruce, Angela BY Hui, Jonathan Irish, Fei-Fei Liu, Bayardo Perez-Ordonez, John Waldron; **Ontario Institute for Cancer Research** Paul C. Boutros, Daryl M. Waggott; **The University of Texas MD Anderson Cancer Center** Jeff Myers, William N. William Jr.; **University of California San Diego** Scott M. Lippman; **University of Miami** Sophie Egea, Carmen Gomez-Fernandez, Lynn Herbert; **University of Michigan** Carol R. Bradford, Thomas E. Carey, Douglas B. Chepeha, Andrea S. Haddad, Tamara R. Jones, Christine M. Komarck, Mayya Malakh, Jonathan B. McHugh, Jeffrey S. Moyer, Ariane Nguyen, Lisa A. Peterson, Mark E. Prince, Laura S. Rozek, Maureen A. Sartor, Evan G. Taylor, Heather M. Walline, Gregory T. Wolf; **University of North Carolina at Chapel Hill** Lori Boice, Bhishamjit S. Chera, William K. Funkhouser, Margaret L. Gulley, Trevor G. Hackman, D. Neil Hayes, Michele C. Hayward, Mei Huang, W. Kimryn Rathmell, Ashley H. Salazar, William W. Shockley, Carol G. Shores, Leigh Thorne, Mark C. Weissler, Sylvia Wrenn, Adam M. Zanation; **University of Pittsburgh** Simion I. Chiosea, Brenda Diergaarde, Ann Marie Egloff, Robert L. Ferris, Marjorie Romkes, Raja Seethala; **Vanderbilt University** Brandee T. Brown, Yan Guo, Michelle Pham; **Yale University** Wendell G. Yarbrough

mapped RNA-Seq reads, primarily aligning to viral genes E6 and E7 (Section S1.2, Figure S1.1). The HPV status by mapping of RNA-Seq reads was concordant with the genomic, sequencing, and molecular data and indicated that 36 tumors were HPV(+) and 243 HPV(−). (Section S1.2, Figure S1.1, Data File S1.2). Of 33 oropharyngeal tumors 64% were positive for HPV, compared to 6% of 246 non-oropharyngeal tumors. Molecular HPV signatures were identified using miRNA, DNA methylation, gene expression, and somatic nucleotide substitutions (Section S1.2, Figures S1.1-S1.3). HPV(+) tumors exhibited infrequent mutations in *TP53* or genetic alterations in *CDKN2A*. We evaluated outcome by site, stage, HPV status, molecular subtypes, and putative biomarkers (Section S1.3, Figure S1.4-5). HPV(+) and interestingly patients with HPV(−), *TP53* wild-type tumors demonstrated favorable outcomes compared to *TP53* mutants and 11q13/*CCND1* amplified tumors.

DNA and RNA Structural Alterations

Most tumors demonstrated copy number alterations (CNAs) including losses of 3p and 8p, and gains of 3q, 5p, and 8q chromosomal regions (Figures 1A and S2.1, Section S2) resembling lung squamous cell carcinomas (LUSCs) [5] (Figure 1A , S2.1, S2.2). HNSCC genomes showed high instability with a mean of 141 altered CNAs (amplifications or deletions) from microarray data and 62 structural aberrations (chromosomal fusions) per tumor by “high coverage” whole genome sequencing (n=29) (Section S2.2). We observed 39 regions of recurrent copy number (CN) loss and 23 regions of recurrent CN gain ($q < 0.1$, Data File S2.1,2). Both HPV(+) and (-) tumors harbored recurrent focal amplifications for 3q26/28, a region involving squamous lineage transcription factors *TP63* and *SOX2* and the oncogene *PIK3CA* (Figures 1B, S2.3).

HPV(+) tumors were distinguished by novel recurrent deletions (n=5/36, 14%) and truncating mutations (n=3/36, 8%) of TNF receptor-associated factor 3 (*TRAF3*) gene loss (Figure S2.3,4, Data File S2.1). *TRAF3* is implicated in innate and acquired anti-viral responses [6] including Epstein-Barr, HPV, and HIV [7-9] while loss promotes aberrant NF-κB signaling [10]. While *TRAF3* inactivation has been reported in hematologic malignancies and nasopharyngeal carcinoma [11,12], this is the first evidence linking *TRAF3 to HPV*-associated carcinomas. HPV(+) tumors were also notable for focal amplification of *E2F1* and an intact 9p21.3 region containing the *CDKN2A* gene commonly deleted in HPV(−) tumors.

HPV(−) tumors featured novel co-amplifications of 11q13 (*CCND1*, *FADD*, and *CTTN*) and 11q22 (*BIRC2*, *YAP1*) which also harbor genes implicated in cell death/NF-κB and Hippo pathways. HPV(−) tumors featured novel focal deletions in the Nuclear Set Domain gene (*NSD1)* and tumor suppressor genes (e.g. *FAT1*, *NOTCH1*, *SMAD4*, and *CDKN2A*; Figure S2.3). Recurrent focal amplifications in receptor tyrosine kinases (e.g. *EGFR, ERBB2 and FGFR1*) also predominated in HPV(−) tumors. Interestingly, unsupervised clustering analysis of CNAs identified a mutually exclusive subset of predominantly oral cavity tumors with reduced CNAs, a pattern recently described in cancer as “M” class (tumors driven by mutation rather than CNA) (Figure 1B) [13]. This subset in particular harbored a novel 3 gene pattern of activating mutations in *HRAS*, frequently with inactivating *CASP8* mutations, and wild type *TP53*. We confirmed a previously reported favorable clinical outcome in tumors with few CNAs [14]. The three gene constellation of wild type *TP53* with mutant *HRAS* and

CASP8 suggested an alternative tumorigenesis pathway involving RAS and/or alterations in cell death/NF-κB [15]. Unsupervised analysis also suggested that clustering was a function of chromosome 7 amplification (including the *EGFR* locus) in a manner that largely excluded HPV(+) tumors.

To detect additional structural alterations, we interrogated whole genome and RNA-Seq data (Section S3, Data File S3.1, Figure S3.1). Known fusion oncogenes reported in solid tumors including those involving the *ALK*, *ROS*, or *RET* genes were not observed in HNSCC. Previously reported *FGFR3-TACC3* fusions [5] were present in two HPV(+) tumors (Figure S3.2). Only one of 279 patients showed evidence of the vIII isoform of *EGFR*, previously described in HNSCC (Figure S3.3) [16]. While our investigation did not identify additional novel oncogenic fusions, several tumors demonstrated exon 1 of *EGFR* or *FGFR3* fused to non-recurrent partners, suggesting potential promoter swaps for the partner genes (Data File S3.1). A low prevalence of an alternate *MET* transcript with skipped exon 14 was identified in two HPV(−) tumors (Figure S3.4); this finding was reported to be an activating event in non-small cell lung cancer [17]. Structural alterations (homozygous deletions, intra- and inter-chromosomal fusions) were more commonly associated with loss of function in tumor suppressor genes, most prominently *CDKN2A* (Figure S3.5-6), followed by *TP53*, *RB1*, *NOTCH1*, and *FAT1* (Figures S3.7-S3.9) than protein coding fusion events. RNA-Seq data (Data File S3.3) demonstrated evidence of alterative splicing in genes not previously described in HNSCC including kallikrein 12 (*KLK12*) (Figure S3.11), as well as genes such as *TP63* with known importance in HNSCC (Figure S3.12).

By DNA analysis, most HPV(+) tumors demonstrated clear evidence of host genome integration, usually in a single genomic location per sample and almost always in association with amplifications of the host genome (Figure S3.10, Data File S3.2). Interrogation of RNA transcripts confirmed transcription across the viral-human integration locus. However, none of the genes involved were recurrent which suggests a single driver mechanism related to HPV integration. Similarly, none of the integration sites involved the *MYC* gene as reported in HPV(+) cell lines[18].

Somatic Mutations

Whole exome sequencing identified somatically mutated genes, many located in regions of CNAs and annotated in the COSMIC database (Figure 2) [19]. The mean sequencing coverage across targeted bases was 95X, with 82% of target bases above 30X coverage. In 279 samples, 12,159 synonymous somatic variants, 37,061 non-synonymous somatic variants, and 2,579 germline single base substitutions from dbSNP [20] were detected (Section S4). Targeted re-sequencing of 394 unique regions (Figure S4.1) validated 99% of mutations. Interrogation of RNA for expression of the mutated alleles confirmed the variant in 86% of cases (S3.2, Figure S3.1). In contrast to prior reports, the mutation rates did not differ by HPV status, although transversions at CpG sites were more frequent in HPV(−) tumors and a predominance of TpCmutations were noted in HPV(+) cases (Figure S1.1) [3]. Mutations were statistically enriched in 11 genes (Figure 2). Among inactivating mutations (premature termination of the protein by nonsense, frameshift, or splice site mutations), four genes segregated exclusively or predominantly in HPV(−) tumors. Two were associated with cell

cycle and survival (*CDKN2A* (p<0.01) and *TP53* (p<0.01)) and two were linked to Wnt/β-catenin signaling (*FAT1* (p<0.01) and *AJUBA* (p=0.14)) [21,22]. We observed *TP53* mutation among HPV(−) samples at rates higher (86%) than have been previously reported [23], while only 1 of 36 HPV(+) cases had a non-synonymous *TP53* mutation. Previously unreported somatic mutations and deletions of *AJUBA* were primarily 5' inactivating events and clustered missense mutations in the functional LIM domain (Figure S4.2). *AJUBA* is a centrosomal protein that regulates cell division, vertebrate ciliogenesis, and left-right axis determination [24]. Additionally, *AJUBA* is subject to EGFR-RAS-MAPK-dependent phosphorylation and implicated in Hippo growth and regeneration pathways conserved from Drosophila to mammals [25,26], in ATR-mediated DNA damage response, [27] and tumor invasion and migration [28].

A frequently mutated novel gene, the nuclear receptor binding SET domain protein 1 *(NSD1)*, was identified in 33 HNSCCs. Alterations included inactivating mutations (n=29) and focal homozygous deletions (n=4). *NSD1* is a Histone H3K36 methyltransferase, similar to *SETD2*, which is frequently mutated in the clear cell variant of renal cell carcinoma, and associated with DNA hypomethylation [29]. Germline carriers of inactivating mutations in *NSD1* are associated with craniofacial abnormalities (Sotos syndrome), and malignancies including squamous carcinoma, implicating *NSD1* as a tumor suppressor gene [30]. Interestingly, *NSD1* functions as an oncogene when fused to nucleoporin-98 (*NUP98*) t(5;11)(q35;p15.5) in hematologic cancers with elevated H3K36me3 levels at *HOXA* genes and accompanying transcriptional activation [31]. Translocations involving other dedicated H3K36 methyltransferase genes including *WHSC1* / *MMSET* / *NSD2* are reported in 20% of multiple myelomas. In contrast *NSD1* loss has been associated with sporadic non-melanoma skin cancers [32]. Significant inactivating mutations were found in genes linked to squamous differentiation including in *NOTCH1* (19%), and other non-significant (NS) family members (*NOTCH2* 9%, and *NOTCH3* 5%, q>0.1, NS), and the *TP63* target gene *ZNF750* (4%, q>0.1, NS) which falls in a significantly deleted peak at 17q25.3. The analysis identified additional mutations including *TRAF3*, *RB1*, *NFE2L2*, among others with q-values <1(NS). The frequently mutated apoptosis gene *CASP8* displayed clustered missense and other inactivating mutations in the first death effector, intron, and caspase peptidase domains. Statistically significant mutations in *KMT2D* (aka *MLL2*) and *HLAA* could contribute to defective immunosurveillance. Of known oncogenes, only *PIK3CA* achieved (q <0.01) statistical significance. Approximately one-fourth of the mutated *PIK3CA* cases displayed concurrent amplification, with an additional 20% of tumors containing focal amplification without evidence of mutation. Seventy-three percent of *PIK3CA* mutations localized to E542K, E545K, and H1047R/L hotspots that promote activation, with the remaining mutations of uncertain function. Recurrent activating mutations of *HRAS* in the GTPase domain in residues 11-13 approached statistical significance (q=0.2).

We extended our unsupervised genome-wide analysis of significantly mutated genes as well as genes reported in COSMIC to a subgroup analysis by anatomic sites, tumor vs. normal status, HPV status, and four previously validated gene expression subtypes (Section S5, Figures S5.1-4, Data File S4.1, 5.1-4) [33,34] Additional mutations included *TRAF3*, *RB1*, *NFE2L2*, among others with q-values <1, and we observed statistical evidence for mutations

of *HRAS* (q=0 in COSMIC subset) and other genes. Sporadic inactivating mutations and deletions of *TGFBR2* were identified primarily in oral cavity tumors, consistent with its role in promoting squamous tumorigenesis in mouse models [35]. Investigating COSMIC database mutations focused attention on the significant deletion peak at 4q31.3 containing the gene *FBXW7*, a ubiquitin ligase targeting *cyclin E* and *NOTCH* genes, in which we identified mutations that included recurrent R505G/L substitutions (n=14). Genes with at least one identical mutation previously reported in COSMIC include *SCN9A, CHEK2, PTCH1,* and *PIK3R1*. We further focused on somatic alterations and protein expression that represent plausible therapeutic targets (Figure 3) (Section S6, Figures S6.1,2, Data File S6.1,2, Section S7).

Integrated Genome Analysis and Pathways

Correlative genetic alteration analysis identified numerous pairwise significant findings (Section S7, Figure S7.1). In particular, co-amplification of 11q13 harboring *CCND1*, *FADD*, and *CTTN* and a narrow segment of 11q22 harboring the genes with equal evidence for *YAP1* and *BIRC2* was further characterized (Figure S7.2). Chromosome 11q22 was focally but rarely amplified in the absence of co-amplification of 11q13. This novel finding suggests that the selection pressure for this co-amplification stems from BIRC2's interaction with FADD and the caspase cascade that inhibits cell death. Interestingly, the vast majority of tumors with the 11q13 amplification had large deletions in the telomeric region of 11q22 including other genes known to be important in cell death in cancer including *ATM* and the *caspases 1*, *4*, *5*, and *12*. 11q13 amplification was anti-correlated with *CASP8* mutations, suggesting an alternate function of *CASP8* and *FADD* in cell death/NF-κB activation [36].

We investigated whether clinical factors, single gene alterations and statistically significant pairwise gene correlations (Figure S7.1, Data File S7.1) might segregate previously defined molecular subtypes and/or anatomic sub-sites (Data File S5.1-4). We confirmed reported gene expression subtypes (Atypical (24%), Mesenchymal (27%), Basal (31%), and Classical (18%)), and assessed the subtypes for enrichment of somatic alterations (Data File S7.1) [33,34]. Notably, *TP53* mutation, *CDKN2A* loss of function, chromosome 3q amplification, alteration of oxidative stress genes (*KEAP1, NFE2L2,* or *CUL3*), heavy smoking history (Table S1.1), and larynx sub-site co-occurred in the majority of Classical subtype tumors (Figure 4A, Section S7.2), similar to LUSC (Figure S5.1, 2)[5]. Collectively, these findings suggest that the *NFE2L2* oxidative stress pathway is a tobacco-related signature across anatomic tumor sites. In contrast, the Basal subtype demonstrated inactivation of *NOTCH1* with intact oxidative stress signaling and fewer alterations of chromosome 3q. Analysis of the 3q locus highlighted a dramatic relative decrease of *SOX2* expression in Basal tumors relative to all other HNSCC and tumor adjacent normal samples (Figure S5.4) supporting the interaction of transcription factors *SOX2, TP63, NFE2L2,* and *NOTCH1* as driving differences between expression subtypes. Additionally, the Basal subtype included most tumors with the *HRAS-CASP8* co-mutation and the majority of co-amplified 11q13/q22 tumors. These findings along with *HRAS* mutations implicate disrupted cell death as a major alteration in this subtype (Figure S7.2) [37]. The Atypical subtype was characterized by a lack of chromosome 7 amplifications (Figure S5.3), enrichment of HPV(+) tumors with activating mutations in exon 9 of the *PIK3CA* helicase domain. In

contrast, the Mesenchymal subtype showed high levels of alteration in innate immunity genes, in particular high NK cell marker *CD56* expression and a low frequency of HLA class I mutations (Figure S7.3). Among the significantly mutated genes, *TP53* ($p<0.001$), *CASP8* ($p=0.01$), *NSD1* ($p=0.01$), and *CDKN2A* (0.06) were the most differentially mutated across anatomic sites (Data File S4.1). The majority of *CASP8* mutations (22/24, 92%) were in oral cavity tumors, while *TP53*, *NSD1*, and *CDKN2A* demonstrated decreased mutation rates in oropharyngeal tumors relative to other sites.

Unsupervised analysis of gene expression by HPV status and of reverse phase protein arrays (RPPA, Section S6), DNA methylation (Section S8), and miRNA platforms (Section S9, Table S9.1, Figure S7.4-9, Data File S7.1) showed high correlation across platforms ($p<0.01$, Figure 4, S7.9, Data File S7.2) and coordinated alterations of genes including the epithelial-mesenchymal transition (EMT) signature (Figures S7.4, S7.7,8) [38]. However, within the broader cross-platform agreement, individual unsupervised clustering of miRNA, RPPA, and DNA methylation data provided insight into the association of molecular subtypes with single gene alterations. The most striking example was the detection of a hypomethylation and loss of function mutations of *NSD1*, and wild type *NOTCH1* in Atypical and Classical gene expression subtypes (Figure 4B, Table S7.1).

Supervised analyses detected genomic features (miRNA, gene expression, and DNA methylation) associated with anatomic site (Figure S5.5-8, Data File S5.1-4). A supervised integrated analysis identified target genes that are inversely regulated by miRNAs in HNSCC (Section S7.4). Among these miRNA-mRNA networks, let-7c-5p and miR-100-5p exhibited a correlation between low copy number and expression. Let-7c-5p and miR-100-5p were decreased in tumors compared to normal (Figure S7.10). For these miRNAs, deletion was highly associated with increased expression of target genes, including the cell cycle regulator *CDK6*, transcription factor *E2F1* [39] mitosis regulator *PLK1* [40], and transcription factor *HMGA2* (Figures S7.10, Tables S7.2, 3) [41].

Integrative bioinformatics analysis identified a limited number of pathways targeted by frequent genome alterations (Figure 5; Section S7, Figure S7.11-15, Data File S7.3). Among receptor tyrosine kinases, *EGFR/ERBB2* or *FGFR1/3* alterations are the most frequent. Among downstream targets of the RTK/RAS/PI3K pathway, *PIK3CA* dominates with occasional *HRAS* and *PTEN* alterations. Further downstream, nearly every tumor has alteration of genes governing the cell cycle. The tumor suppressors *TP53*, *CDKN2A*, oncogenes *CCND1*, *MYC*, and the newly identified miR let-7c, are most often altered in HPV(−) tumors, while viral *E6/7* and *E2F1* predominate in HPV(+) cases. In addition, we report frequent alterations in genes involved in cell death, NF-κB-mediated survival, or immunity pathways [15,36]. Co-amplification of *FADD*+/−*BIRC2*, or *CASP8*+/−*HRAS* mutations define exclusive HPV(−) subsets, while *TRAF3* loss characterizes an HPV(+) subset. These alterations along with *PIK3CA* and *TP63* converge upon NF-κB transcription factors that promote cell survival, migration, inflammation and angiogenesis [42,43]. Additionally, *TRAF3* and/or *HLA* loss are implicated in deregulation of innate antiviral and adaptive anti-tumor immunity [44,45]. Further alterations of *NOTCH*, *TP63*, and other genes in HPV(−) tumors (*FAT1*, *AJUBA*) recently linked functionally to beta-catenin (*CTNNB1*) are also detected [21,22,46]. Finally, we highlight a previously underappreciated role for a key

transcription factor regulator of oxidative stress, *NFE2L2*, and its protein complex partners *CUL3* and *KEAP1* in HPV(−) HNSCC.

Conclusion

The TCGA study represents the most comprehensive integrative genomic analysis of HNSCC. Loss of *TRAF3*, activating mutations of *PIK3CA*, and amplification of *E2F1* in HPV(+) oropharyngeal cancers point to aberrant activation of NF-κB, other oncogenic pathways, and cell cycle, as critical in the pathogenesis and development of new targeted therapies for these tumors. In HPV(−) HNSCC mutually exclusive subsets harboring amplicons on 11q with *CCND1*, *FADD*, *BIRC2* and *YAP1*, or concurrent mutations of *CASP8* with *HRAS*, also target cell cycle, death, NF-κB and other oncogenic pathways. Recent studies predict that the inactivation of *AJUBA*, as well as *FAT1* and *NOTCH1* may converge to uncheck Wnt/β−catenin signaling, implicated in deregulation of cell polarity and differentiation. The 3q amplicon found in both HPV(+) and (-) HNSCC includes transcription factors *TP63*, *SOX2* and signal molecule *PIK3CA*, which are also implicated in homeostasis of epithelial stem cells and differentiation. Among these, the biologic function and agents targeting BIRCs, PI3K, Wnt/β−catenin and NOTCH are under investigation. Collectively, these findings provide new insights into HNSCC and suggest that shared and unique alterations might be leveraged to accelerate progress in prevention and therapy across tumor types.

Supplementary Material

Refer to Web version on PubMed Central for supplementary material.

Acknowledgements

This study was supported by NIH grants: P50CA097190, P50CA16672, U54 HG003273, U54 HG003067, U54 HG003079, U24 CA143799, U24 CA143835, U24 CA143840, U24 CA143843, U24 CA143845, U24 CA143848, U24 CA143858, U24 CA143866, U24 CA143867, U24 CA143882, U24 CA143883, U24 CA144025, RO1 CA 095419. Supported by the Bobby F. Garrett Cancer Foundation and NIDCD Intramural Projects ZIA-DC-000016, 73 and 74.

References

1. Ferlay J, et al. Estimates of worldwide burden of cancer in 2008: GLOBOCAN 2008. International journal of cancer. Journal international du cancer. 2010; 127:2893–2917. doi:10.1002/ijc.25516. [PubMed: 21351269]
2. Ang KK, et al. Human papillomavirus and survival of patients with oropharyngeal cancer. The New England journal of medicine. 2010; 363:24–35. doi:10.1056/NEJMoa0912217. [PubMed: 20530316]
3. Stransky N, et al. The mutational landscape of head and neck squamous cell carcinoma. Science. 2011; 333:1157–1160. doi:10.1126/science.1208130. [PubMed: 21798893]
4. Agrawal N, et al. Exome sequencing of head and neck squamous cell carcinoma reveals inactivating mutations in NOTCH1. Science. 2011; 333:1154–1157. doi:10.1126/science.1206923. [PubMed: 21798897]
5. Singh D, et al. Transforming fusions of FGFR and TACC genes in human glioblastoma. Science. 2012; 337:1231–1235. doi:10.1126/science.1220834. [PubMed: 22837387]
6. Oganesyan G, et al. Critical role of TRAF3 in the Toll-like receptor-dependent and -independent antiviral response. Nature. 2006; 439:208–211. doi:10.1038/nature04374. [PubMed: 16306936]

7. Karim R, et al. Human papillomavirus (HPV) upregulates the cellular deubiquitinase UCHL1 to suppress the keratinocyte's innate immune response. PLoS pathogens. 2013; 9:e1003384. doi: 10.1371/journal.ppat.1003384. [PubMed: 23717208]
8. Eliopoulos AG, et al. CD40-induced growth inhibition in epithelial cells is mimicked by Epstein-Barr Virus-encoded LMP1: involvement of TRAF3 as a common mediator. Oncogene. 1996; 13:2243–2254. [PubMed: 8950992]
9. Imbeault M, et al. Acquisition of host-derived CD40L by HIV-1 in vivo and its functional consequences in the B-cell compartment. Journal of virology. 2011; 85:2189–2200. doi:10.1128/JVI.01993-10. [PubMed: 21177803]
10. Ni CZ, et al. Molecular basis for CD40 signaling mediated by TRAF3. Proceedings of the National Academy of Sciences of the United States of America. 2000; 97:10395–10399. [PubMed: 10984535]
11. Chung GT, et al. Constitutive activation of distinct NF-kappaB signals in EBV-associated nasopharyngeal carcinoma. The Journal of pathology. 2013 doi:10.1002/path.4239.
12. Annunziata CM, et al. Frequent engagement of the classical and alternative NF-kappaB pathways by diverse genetic abnormalities in multiple myeloma. Cancer cell. 2007; 12:115–130. doi: 10.1016/j.ccr.2007.07.004. [PubMed: 17692804]
13. Ciriello G, et al. Emerging landscape of oncogenic signatures across human cancers. Nature genetics. 2013; 45:1127–1133. doi:10.1038/ng.2762. [PubMed: 24071851]
14. Smeets SJ, et al. Genetic classification of oral and oropharyngeal carcinomas identifies subgroups with a different prognosis. Cellular oncology : the official journal of the International Society for Cellular Oncology. 2009; 31:291–300. doi:10.3233/CLO-2009-0471. [PubMed: 19633365]
15. Mayo MW, et al. Requirement of NF-kappaB activation to suppress p53-independent apoptosis induced by oncogenic Ras. Science. 1997; 278:1812–1815. [PubMed: 9388187]
16. Sok JC, et al. Mutant epidermal growth factor receptor (EGFRvIII) contributes to head and neck cancer growth and resistance to EGFR targeting. Clinical cancer research : an official journal of the American Association for Cancer Research. 2006; 12:5064–5073. doi: 10.1158/1078-0432.CCR-06-0913. [PubMed: 16951222]
17. Kong-Beltran M, et al. Somatic mutations lead to an oncogenic deletion of met in lung cancer. Cancer research. 2006; 66:283–289. doi:10.1158/0008-5472.CAN-05-2749. [PubMed: 16397241]
18. Popescu NC, DiPaolo JA, Amsbaugh SC. Integration sites of human papillomavirus 18 DNA sequences on HeLa cell chromosomes. Cytogenetics and cell genetics. 1987; 44:58–62. [PubMed: 3028716]
19. Forbes SA, et al. The Catalogue of Somatic Mutations in Cancer (COSMIC). Current Protocols in Human Genetics. 2008 Chapter 10, Unit 10 11, doi:10.1002/0471142905.hg1011s57.
20. Sherry ST, et al. dbSNP: the NCBI database of genetic variation. Nucleic acids research. 2001; 29:308–311. [PubMed: 11125122]
21. Morris LG, et al. Recurrent somatic mutation of FAT1 in multiple human cancers leads to aberrant Wnt activation. Nature genetics. 2013; 45:253–261. doi:10.1038/ng.2538. [PubMed: 23354438]
22. Haraguchi K, et al. Ajuba negatively regulates the Wnt signaling pathway by promoting GSK-3beta-mediated phosphorylation of beta-catenin. Oncogene. 2008; 27:274–284. doi:10.1038/sj.onc.1210644. [PubMed: 17621269]
23. Forbes SA, et al. The Catalogue of Somatic Mutations in Cancer (COSMIC). Curr Protoc Hum Genet. 2008 Chapter 10, Unit 10 11, doi:10.1002/0471142905.hg1011s57.
24. Nagai Y, et al. The LIM protein Ajuba is required for ciliogenesis and left-right axis determination in medaka. Biochemical and biophysical research communications. 2010; 396:887–893. doi: 10.1016/j.bbrc.2010.05.017. [PubMed: 20457130]
25. Sun G, Irvine KD. Ajuba family proteins link JNK to Hippo signaling. Science signaling. 2013; 6:ra81. doi:10.1126/scisignal.2004324. [PubMed: 24023255]
26. Reddy BV, Irvine KD. Regulation of Hippo signaling by EGFR-MAPK signaling through Ajuba family proteins. Developmental cell. 2013; 24:459–471. doi:10.1016/j.devcel.2013.01.020. [PubMed: 23484853]

27. Kalan S, Matveyenko A, Loayza D. LIM protein Ajuba participates in the repression of the ATR-mediated DNA damage response. Frontiers in genetics. 2013; 4:95. doi:10.3389/fgene.2013.00095. [PubMed: 23755068]
28. Nola S, et al. Ajuba is required for Rac activation and maintenance of E-cadherin adhesion. The Journal of cell biology. 2011; 195:855–871. doi:10.1083/jcb.201107162. [PubMed: 22105346]
29. Comprehensive molecular characterization of clear cell renal cell carcinoma. Nature. 2013; 499:43–49. doi:10.1038/nature12222. [PubMed: 23792563]
30. Fickie MR, et al. Adults with Sotos syndrome: review of 21 adults with molecularly confirmed NSD1 alterations, including a detailed case report of the oldest person. American journal of medical genetics. Part A. 2011; 155A:2105–2111. doi:10.1002/ajmg.a.34156. [PubMed: 21834047]
31. Wang GG, Cai L, Pasillas MP, Kamps MP. NUP98-NSD1 links H3K36 methylation to Hox-A gene activation and leukaemogenesis. Nature cell biology. 2007; 9:804–812. doi:10.1038/ncb1608. [PubMed: 17589499]
32. Quintana RM, et al. A transposon-based analysis of gene mutations related to skin cancer development. The Journal of investigative dermatology. 2013; 133:239–248. doi:10.1038/jid.2012.245. [PubMed: 22832494]
33. Chung CH, et al. Molecular classification of head and neck squamous cell carcinomas using patterns of gene expression. Cancer cell. 2004; 5:489–500. [PubMed: 15144956]
34. Walter V, et al. Molecular subtypes in head and neck cancer exhibit distinct patterns of chromosomal gain and loss of canonical cancer genes. PloS one. 2013; 8:e56823. doi:10.1371/journal.pone.0056823. [PubMed: 23451093]
35. Lu SL, et al. Loss of transforming growth factor-beta type II receptor promotes metastatic head-and-neck squamous cell carcinoma. Genes & development. 2006; 20:1331–1342. doi:10.1101/gad.1413306. [PubMed: 16702406]
36. Oberst A, Green DR. It cuts both ways: reconciling the dual roles of caspase 8 in cell death and survival. Nature reviews. Molecular cell biology. 2011; 12:757–763. doi:10.1038/nrm3214. [PubMed: 22016059]
37. Park SJ, et al. Opposite role of Ras in tumor necrosis factor-alpha-induced cell cycle regulation: competition for Raf kinase. Biochemical and biophysical research communications. 2001; 287:1140–1147. doi:10.1006/bbrc.2001.5713. [PubMed: 11587542]
38. Byers LA, et al. An epithelial-mesenchymal transition gene signature predicts resistance to EGFR and PI3K inhibitors and identifies Axl as a therapeutic target for overcoming EGFR inhibitor resistance. Clinical cancer research : an official journal of the American Association for Cancer Research. 2013; 19:279–290. doi:10.1158/1078-0432.CCR-12-1558. [PubMed: 23091115]
39. Wong JV, Dong P, Nevins JR, Mathey-Prevot B, You L. Network calisthenics: control of E2F dynamics in cell cycle entry. Cell Cycle. 2011; 10:3086–3094. [PubMed: 21900750]
40. Sanhaji M, et al. Polo-like kinase 1 inhibitors, mitotic stress and the tumor suppressor p53. Cell Cycle. 2013; 12:1340–1351. doi:10.4161/cc.24573. [PubMed: 23574746]
41. Morishita A, et al. HMGA2 is a driver of tumor metastasis. Cancer research. 2013; 73:4289–4299. doi:10.1158/0008-5472.CAN-12-3848. [PubMed: 23722545]
42. Bancroft CC, et al. Effects of pharmacologic antagonists of epidermal growth factor receptor, PI3K and MEK signal kinases on NF-kappaB and AP-1 activation and IL-8 and VEGF expression in human head and neck squamous cell carcinoma lines. International journal of cancer. Journal international du cancer. 2002; 99:538–548. doi:10.1002/ijc.10398. [PubMed: 11992543]
43. Yang X, et al. DeltaNp63 versatilely regulates a Broad NF-kappaB gene program and promotes squamous epithelial proliferation, migration, and inflammation. Cancer research. 2011; 71:3688–3700. doi:10.1158/0008-5472.CAN-10-3445. [PubMed: 21576089]
44. Keating PJ, et al. Frequency of down-regulation of individual HLA-A and -B alleles in cervical carcinomas in relation to TAP-1 expression. British journal of cancer. 1995; 72:405–411. [PubMed: 7640226]
45. Esteban F, et al. Lack of MHC class I antigens and tumour aggressiveness of the squamous cell carcinoma of the larynx. British journal of cancer. 1990; 62:1047–1051. [PubMed: 2257212]

46. Dotto GP. Crosstalk of Notch with p53 and p63 in cancer growth control. Nature reviews. Cancer. 2009; 9:587–595. doi:10.1038/nrc2675.

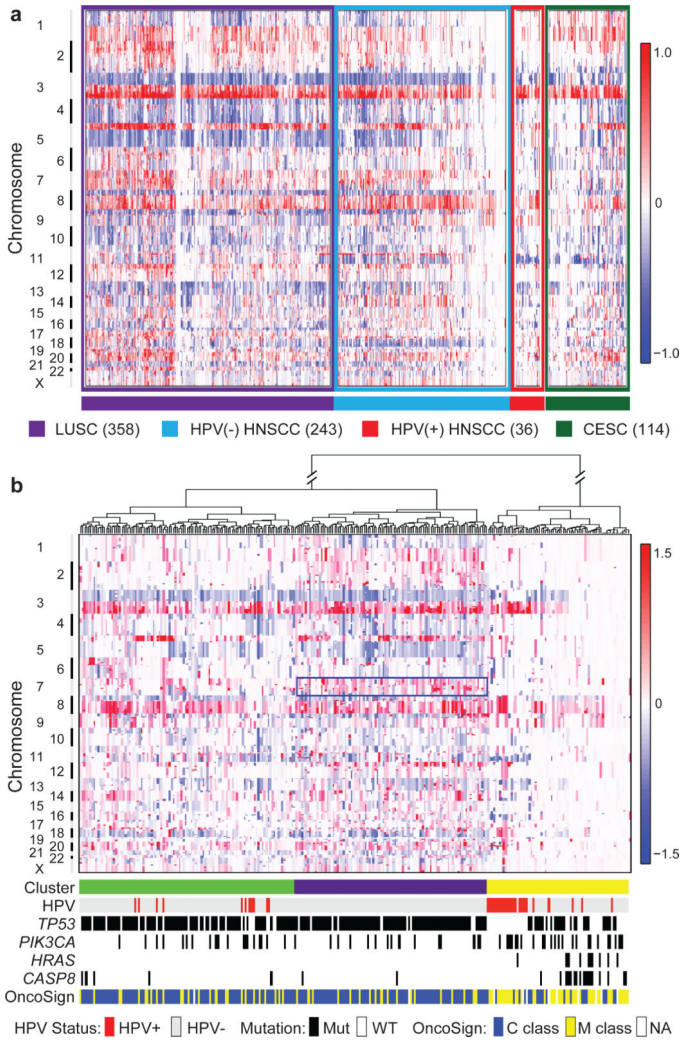

Figure 1.

A. Copy number alterations by anatomic site and HPV status for squamous cancers. Lung squamous cell carcinoma (LUSC, n = 358), cervical squamous cell carcinoma (CESC, n = 114). B. Unsupervised analysis of copy number alteration of HNSCC (n = 279) with associated characteristics. The Rectangle indicates chromosome 7 amplifications in the purple cluster.

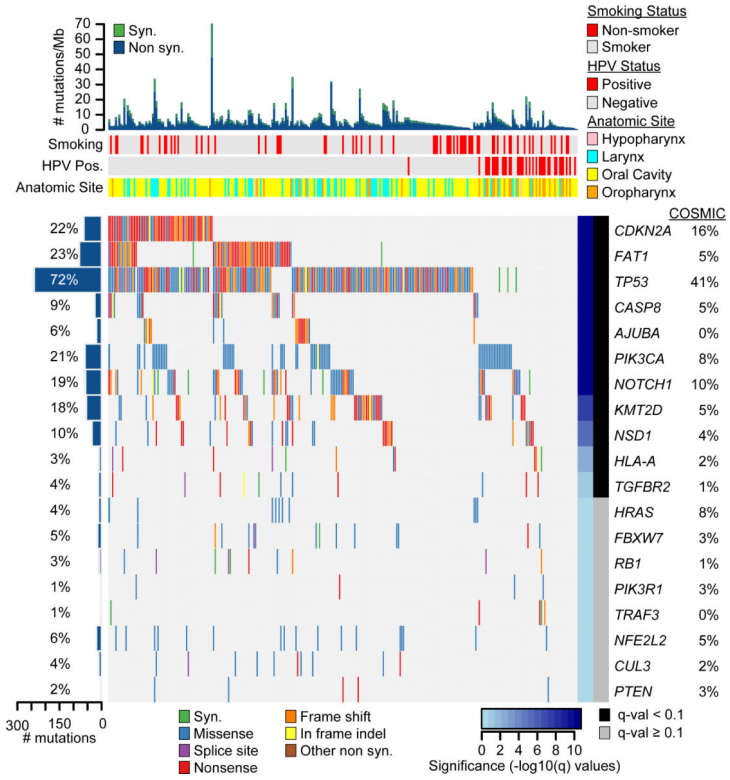

Figure 2.

Significantly mutated genes in HNSCC. Genes (rows) with significantly mutated genes (MutSigCV q <0.1) ordered by q-value; additional genes with trends towards significance are also shown. Samples (columns, n = 279) are arranged to emphasize mutual exclusivity among mutations. Left, mutation percentage in TCGA; Right, mutation percentage in COSMIC (“upper aerodigestive tract” tissue); Top, overall number of mutations per megabase. Color coding indicates mutation type.

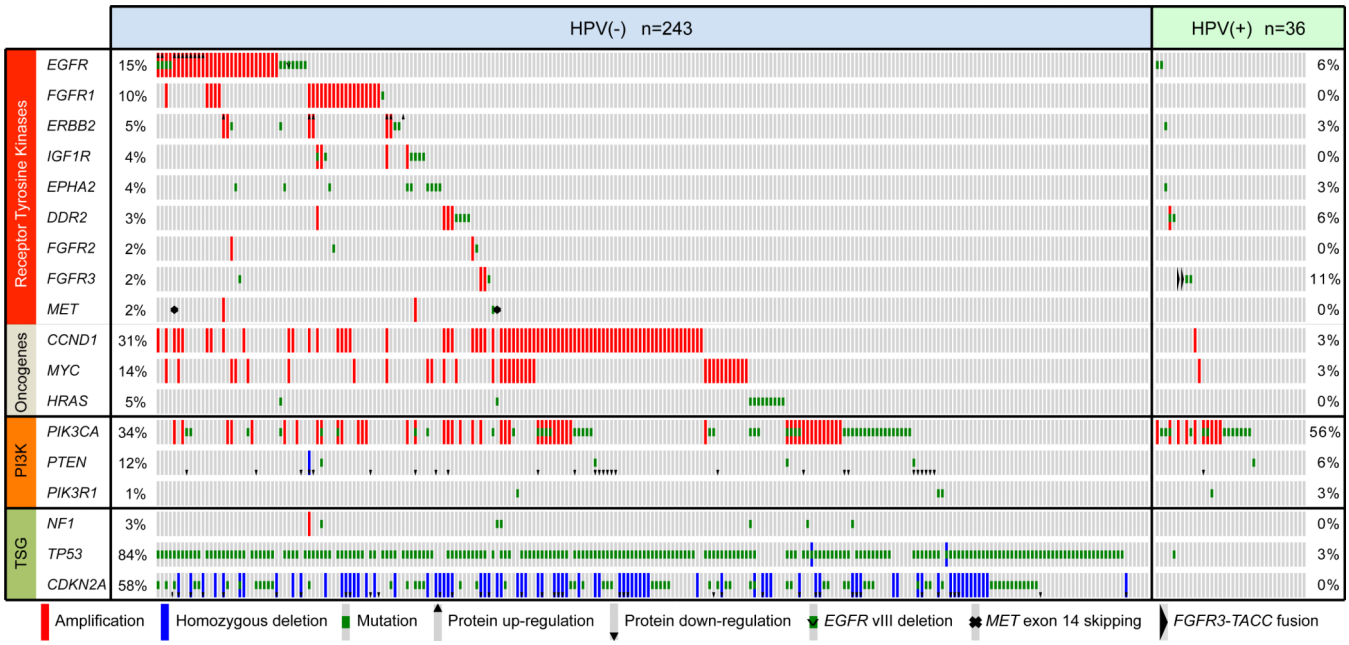

Figure 3.

Candidate therapeutic targets and driver oncogenic events. Alteration events for key genes are displayed by sample (n = 279). TSG, tumor suppressor gene.

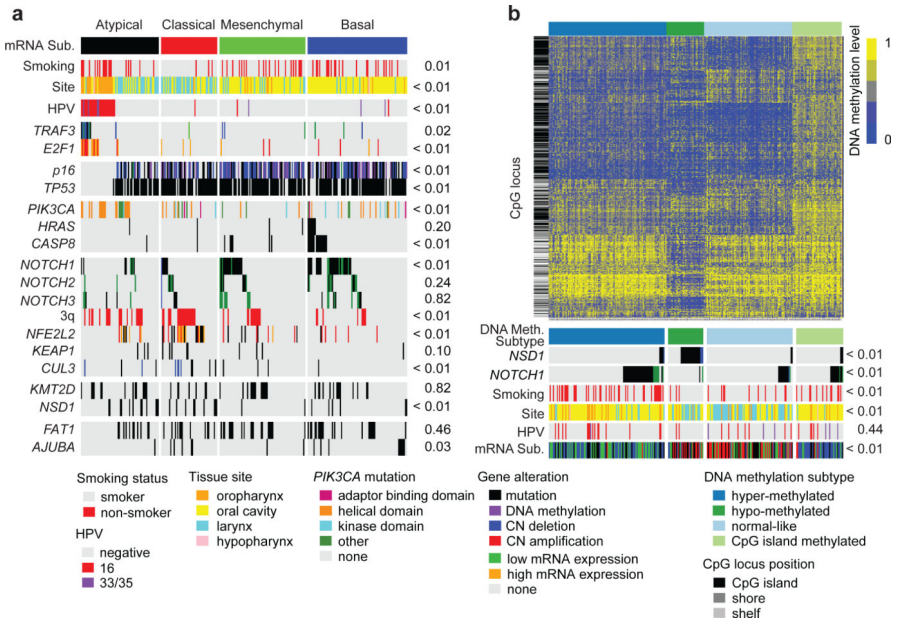

Figure 4.

Integrated analysis of genomic alterations. Samples (n = 279) are displayed in columns and grouped by (A) gene expression subtype or (B) methylation subtype. Unadjusted two-sided Fisher's exact test p-values assess the association of each genomic alteration. Methylation probe location of CpG islands, shores and shelves are shown on the left of panel B.

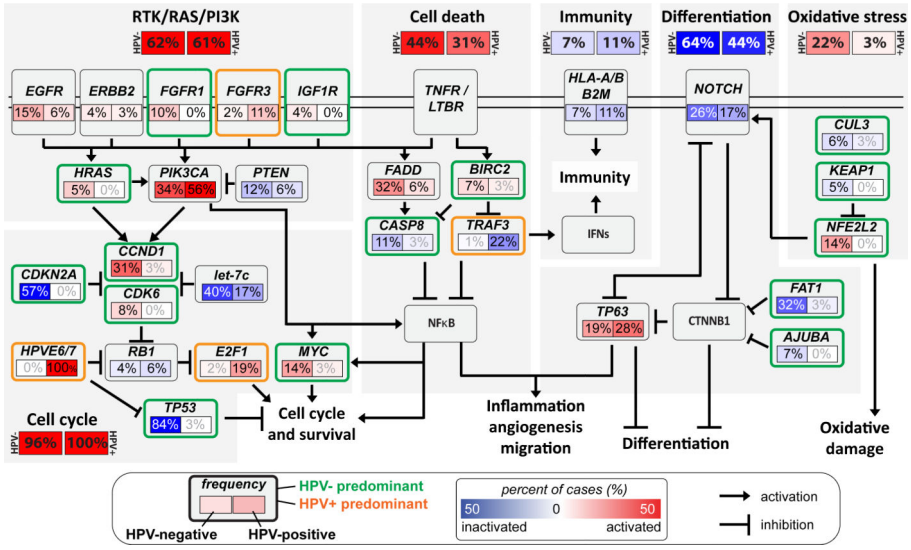

Figure 5.

Deregulation of signaling pathways and transcription factors. Key affected pathways, components, and inferred functions, are summarized in the main text and Section S7 for n = 279 samples. The frequency (%) of genetic alterations for HPV(−)and HPV(+)tumors are shown separately within sub-panels and highlighted. Also see Figure S7.15, Parts I and II. Pathway alterations include homozygous deletions, focal amplifications, and somatic mutations. Activated and inactivated pathways/genes, and activating or inhibitory symbols are based on predicted effects of genome alterations and/or pathway functions.